Monthly Notices
of the
ROYAL ASTRONOMICAL SOCIETY

Mon. Not. R. Astron. Soc. **416,** 2869–2881 (2011) doi:10.1111/j.1365-2966.2011.19235.x

The host galaxies of radio-loud active galactic nuclei: colour structure

E. J. A. Mannering,★ D. M. Worrall and M. Birkinshaw

H.H. Wills Physics Laboratory, University of Bristol, Tyndall Avenue, Bristol BS8 1TL

Accepted 2011 June 13. Received 2011 June 1; in original form 2011 January 11

ABSTRACT

We construct a sample of 3516 radio-loud host galaxies of active galactic nuclei (AGN) from the optical Sloan Digital Sky Survey and Faint Images of the Radio Sky at Twenty cm. These have 1.4-GHz luminosities in the range 10^{23}–10^{25} W Hz^{-1}, span redshifts $0.02 < z < 0.18$, are brighter than $r^*_{\rm petro} < 17.77$ mag and are constrained to 'early-type' morphology in colour space ($u^* - r^* > 2.22$ mag). Optical emission line ratios (at $>3\sigma$) are used to remove type 1 AGN and star-forming galaxies from the radio sample using Baldwin–Phillips–Terlevich diagnostics. For comparison, we select a sample of 35 160 radio-quiet galaxies with the same r^*-band magnitude–redshift distribution as the radio sample. We also create comparison radio and control samples derived by adding the NRAO VLA Sky Survey (NVSS) to quantify the effect of completeness on our results.

We investigate the effective radii of the surface brightness profiles in the SDSS r and u bands in order to quantify any excess of blue colour in the inner region of radio galaxies. We define a ratio $R = r_e(r)/r_e(u)$ and use maximum likelihood analysis to compare the average value of R and its intrinsic dispersion between both samples. R is larger for the radio-loud AGN sample as compared to its control counterpart, and we conclude that the two samples are not drawn from the same population at >99 per cent significance. Given that star formation proceeds over a longer time than radio activity, the difference suggests that a subset of galaxies has the predisposition to become radio loud. We discuss host galaxy features that cause the presence of a radio-loud AGN to increase the scale size of a galaxy in red relative to blue light, including excess central blue emission, point-like blue emission from the AGN itself and/or diffuse red emission. We favour an explanation that arises from the stellar rather than the AGN light.

Key words: galaxies: active – galaxies: structure – radio continuum: galaxies.

1 INTRODUCTION

Considerable uncertainties remain as to what controls the apparent link between the activity of active galactic nuclei (AGN) during the time that a black hole is fed and star formation (SF). The accretion disc surrounding a supermassive black hole emits highly energetic radiation and particles, and can form powerful winds and/or collimated, relativistic jets (e.g. van Breugel et al. 2004). The radiation and outflows might then affect the interstellar medium, triggering SF which might be detectable as an excess of blue light from the central regions of galaxies. Alternatively, the activity of the AGN may be sparked by specific events in the galaxy's past. For example, there is morphological evidence that activity in radio galaxies might be triggered by mergers and galaxy interactions (e.g. González Delgado, Tadhunter & Pérez 2006), which in turn could contribute to central blue light through enhanced SF. In either case, we might expect an observable association between AGN activity, for which in this work we use radio loudness as a tracer, with bluer stellar continuum in the central regions of the galaxy.

Previous work has hinted at such a relationship. For example, Mahabal, Kembhavi & McCarthy (1999) examined the central light of 30 radio galaxies as compared to 30 normal galaxies from the Molongo Reference Catalogue and found excess blue light in the inner regions of the radio galaxies as compared with the control sample. This central excess is unrelated to the conventional colour gradient of the broader distribution of stars. Gonzalez-Perez, Castander & Kauffmann (2011) studied colour variations within galaxies from the Sloan Digital Sky Survey Data Release 7 (SDSS DR7; York et al. 2000), finding marginally steeper colour gradients in massive galaxies with nuclear activity, and concluded that this is due to a higher fraction of young stars in their central regions.

In the present paper we expand the work of Mahabal et al. (1999) by combining optical information from SDSS with the Faint Images of the Radio Sky at Twenty cm (FIRST) and NRAO VLA Sky Survey (NVSS) radio surveys (Becker, White & Helfand 1995; Condon et al. 1998) to construct a local ($0.02 < z < 0.18$) sample of powerful radio-loud AGN host galaxies (R-AGN), and a control

★E-mail: l.mannering@bristol.ac.uk

sample of 'normal' early-type ellipticals. We define R as the ratio of SDSS r^* to u^* band de Vaucouleurs effective radii and compare its value between the samples.

The paper is structured as follows. In Section 2 we briefly describe the surveys used to construct our samples. Separation into the radio-loud and control samples is discussed in Section 3. Section 4 outlines the maximum likelihood analysis used to compare the average values of R for the two samples. In Section 5 we present a discussion of our findings in the context of radio-AGN fuelling mechanisms and the properties of the host galaxies. Throughout, we use a flat Λ cold dark matter cosmology with $\Omega_{m_0} = 0.3$ and $\Omega_{\Lambda 0} = 0.7$. We adopt $H_0 = 70\,\mathrm{km\,s^{-1}\,Mpc^{-1}}$.

2 DATA SOURCES

2.1 SDSS

SDSS is an imaging and spectroscopic survey covering $\sim$10 000 deg^2, primarily in the Northern hemisphere. Its seventh data release (SDSS DR7; Abazajian et al. 2009) contains over 350 million entries, of which about one million are confirmed galaxies with spectroscopic follow-up.

In the photometric sample, flux densities are measured simultaneously in five broad-band filters (u, g, r, i, z), with effective wavelengths 3551, 4686, 6165, 7481 and 8931 Å (Fukugita et al. 1996). All magnitudes are given on the AB$_\nu$ system (Oke & Gunn 1983), and are determined using Petrosian apertures (see Blanton et al. 2001; Graham et al. 2005, for a complete definition of the Petrosian system). In common with Ivezić et al. (2002), we refer to SDSS measured magnitudes as u^*, g^*, r^*, i^* and z^* due to the uncertainty in the absolute calibration of the SDSS photometric system, which has been assessed at $\lesssim$0.03 mag (Stoughton & Lupton 2002). For a complete guide to the photometric system, see Fukugita et al. (1996), Gunn et al. (2001) and Stoughton & Lupton (2002).

2.1.1 *Main galaxy sample*

We use the main galaxy survey spectroscopic sample (MGS, Strauss et al. 2002). The MGS algorithm selected extended sources brighter than $r^*_{\mathrm{petro}} = 17.77$ mag with Petrosian half-light surface brightness $\mu_{50} \leq 24.5$ mag arcsec^{-2}, providing $\sim$90 galaxies deg^{-2} (Blanton et al. 2001). Candidate galaxies were then observed spectroscopically. 99.9 per cent of the resulting redshifts have velocity errors $< 30\,\mathrm{km\,s^{-1}}$. The survey is unbiased, except for galaxies with close companions. Around 6 per cent of galaxies satisfying the photometric target criteria were not included for spectroscopic follow-up due to a companion galaxy within the 55 arcsec minimum fibre separation, although some of these galaxies have been subsequently observed. The MGS contains $\sim$680 000 spectroscopically confirmed galaxies. The full target selection is described in Strauss et al. (2002).

We corrected for Galactic extinction using the SDSS 'reddening' parameter, which was derived from maps of the infrared (IR) emission from dust across the sky in accordance with Schlegel, Finkbeiner & Davis (1998). We applied k-corrections using the SDSS-derived 'kcorr' parameter as detailed in Blanton & Roweis (2007). Typical corrections k_u, k_g and k_r were (0–0.4), (0–0.3) and (0–0.1) mag.

2.2 FIRST

The FIRST survey (Becker et al. 1995) utilized the Very Large Array (VLA; at 1.4 GHz in B array) to map the radio sky over $\sim$9000 deg^2 in the Northern hemisphere and in a 2.°5 wide strip along the celestial equator. It has $\sim$8400 deg^2 overlap with SDSS, contains $\sim$97 sources deg^{-2} at the 1 mJy survey threshold and reaches an rms sensitivity of $\sim$0.15 mJy beam^{-1}. In this configuration, the VLA has a synthesized beam of 5.4-arcsec full width at half-maximum (FWHM), providing accurate flux densities for small-scale radio structures, but underestimating the flux densities of sources extended to several arcminutes. At the 1 mJy survey threshold, individual sources have 90 per cent confidence astrometric errors $\lesssim$ 1 arcsec. We adopted a mean spectral index of $\alpha = 0.7$ (where $S_\nu \propto \nu^{-\alpha}$) and obtained rest-frame 1.4-GHz power densities by applying k-corrections assuming the usual form:

$$L_{\nu,\mathrm{rest}} = (1+z)^{(\alpha-1)} S_\nu\, 4\pi D_L^2, \quad (1)$$

where D_L is the luminosity distance.

2.3 NVSS

The NVSS (Condon et al. 1998) mapped the radio sky (at 1.4 GHz in D array) north of -40° declination. The survey is complete down to a point-source flux density of $\sim$ 2.5 mJy. The synthesized beam of 45 arcsec is much larger than FIRST, providing more accurate flux measurements for highly extended sources. Astrometric accuracy ranges from 1 arcsec for bright sources to 7 arcsec for the faintest detections. The entire survey contains over 1.8 million unique sources brighter than 2.5 mJy. k-corrections are applied as in Section 2.2.

3 SAMPLE SELECTION

3.1 Cross-correlation: FIRST–SDSS

We initially derived a FIRST–SDSS sample of radio galaxies and a comparison control sample with no nearby detectable radio counterpart. Fig. 1 shows the distribution of angular separations between SDSS objects and their nearest FIRST counterpart. We find that at $\sim$5 arcsec the distribution becomes dominated by random matches. Hence we adopt a match criterion of 2 arcsec angular separation

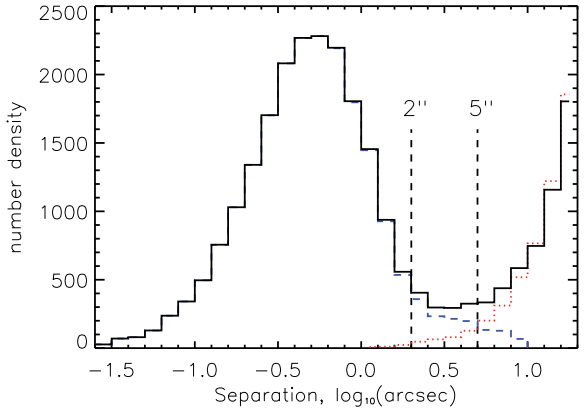

Figure 1. The distribution of angular separations of the matches between FIRST and SDSS, truncated at a 20-arcsec radius (black). The distribution of matches between the FIRST positions offset by 1° and SDSS is shown as a red dotted line. This indicates the number of likely false matches. The net distribution of 'real' matches is shown by the blue dashed line, and our 2 arcsec cut indicates 99.9 per cent efficiency of the matched sample.

to avoid such false matches. Our cross-matched catalogue contains 25 931 galaxies, and we denote this as our preliminary 'radio' sample. All unmatched sources are initial candidates for our control sample of radio-quiet galaxies.

We define our efficiency as the fraction of matches in our radio sample which are physically real (including contamination from line-of-sight false matches, which cannot be accounted for here). In order to evaluate the number of random false matches in our sample, we offset the RA and Dec. of the FIRST sources by 1° and re-matched to our set of 680 056 SDSS galaxies, selecting objects within a 2-arcsec radius. We found on average 58 random matches, corresponding to 0.3 per cent contamination of the FIRST–SDSS match sample (>99 per cent efficiency; Fig. 1, red dotted line).

We also need to know the completeness of our matching criteria – the fraction of correct matches we recover. A factor affecting this is the possible exclusion of large lobe-dominated radio sources (Kimball & Ivezić 2008). Both lobes will be included in the FIRST, but may be excluded in the cross-matched subset for lobe–core distances >2 arcsec, if the core is weak. We estimated ∼8 per cent of real matches between the SDSS subset and FIRST that are excluded from our radio sample, by assuming the radio lobes are outside a 2-arcsec radius from the optical core, but within a 5-arcsec radius (see Fig. 1). Our matching algorithm efficiency and completeness are similar to Kimball & Ivezić (2008), who match FIRST to SDSS DR6 positions within a 2-arcsec radius for sources with $z \leq 2$ (95 per cent efficiency and 98 per cent completeness).[1]

However, we could not account for sources with FIRST lobes >5 arcsec from the optical core or the population of FIRST double-lobed sources with no detectable radio core. Ivezić et al. (2002) cross-correlated all FIRST sources with SDSS, then identified potential double-lobed radio sources with undetected cores,[2] estimating these contribute less than 10 per cent of all radio sources [Best et al. (2005a) estimate ∼5 per cent of their radio-loud AGN sample had no FIRST detection].

Becker et al. (1995) estimated the FIRST catalogue to be 95 per cent complete at 2 mJy and 80 per cent complete down to the survey limit of 1 mJy. Fig. 2 shows integrated radio power against redshift for the preliminary radio sample (25 931 sources). The solid black lines trace the 1 and 2 mJy peak flux density thresholds, the dotted and dashed lines show cuts we applied in redshift and radio power (see Sections 3.3 and 3.4), and the red points are the resultant selection of radio sources. It is noted that for sources that are not well described by an elliptical Gaussian model, the integrated flux density as derived by FIRST may be an inaccurate measure of the true value. Such sources with radio powers corresponding to flux densities below the 1 mJy threshold can be seen in Fig. 2.

We note that although the two cuts improve the sample completeness (all red points are above 1 mJy), many of our sources are below the 2 mJy line, and so our sample completeness cannot be >80 per cent. Combining this with our estimation of completeness in our selection criteria (∼90 per cent), we estimate the actual completeness of our preliminary radio sample to be ∼72 per cent for sources brighter than 1 mJy. The incompleteness is dominated by statistical effects rather than the 10 per cent effect of sources missing due to weak cores.

[1] Kimball & Ivezić (2008) estimate their completeness and efficiency by fitting a Gaussian to the nearest neighbour distribution (representing physical matches) plus a rising linear function (representing random matchings).
[2] Via comparing the mid-points of FIRST pairs to SDSS sources within a separation <90 arcsec and accepted all matches with offsets <3 arcsec.

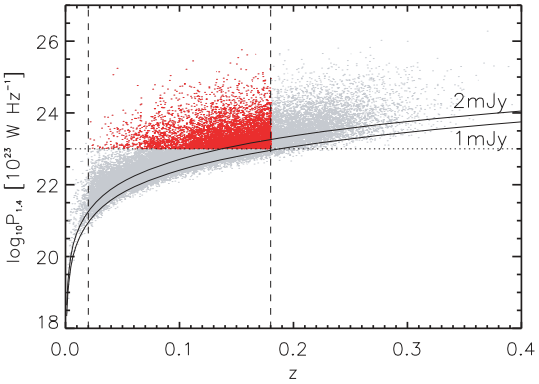

Figure 2. Integrated FIRST radio power versus redshift for the preliminary 'radio' sample (see text). The solid black lines trace peak radio power at the 1 mJy detection threshold and at 2 mJy, the dashed lines denote the redshift limits imposed in Section 3.3 and the dotted line denotes the radio power cut imposed in Section 3.4. The red points are the remaining radio sample after these cuts are applied.

To produce a preliminary control sample, we select sources from the SDSS subset which fall within the same spatial region as FIRST (∼8000 deg^2). We selected all objects from this subset which are not matched to a FIRST source within 2 arcsec of their optical core, providing ∼625 664 radio-quiet galaxies. The efficiency of this sample, based on Fig. 1, is >99.9 per cent (i.e. <1 per cent contamination by radio sources detectable at the FIRST flux density limit), and the sample completeness is >92 per cent.

3.2 Cross-correlation: FIRST–NVSS–SDSS

For FIRST sources substantially larger than 5 arcsec, some flux density is resolved out, leading to an increase in the survey threshold for extended objects and flux density underestimates for larger objects (Lu et al. 2007). Our FIRST–SDSS radio sample is large due to the number of FIRST candidate sources near the 1 mJy survey limit. Its limitations are potential flux density underestimates, and incompleteness to extended radio sources, notably extended, double-lobed sources with no detectable radio core within several arcseconds of its optical counterpart.

To attempt to quantify these limitations, we created a complementary sample of R-AGN using both NVSS and FIRST. Best et al. (2005a) note that the 45-arcsec resolution of NVSS is large enough that ∼99 per cent of all radio sources are contained within a single component, allowing for a higher sample completeness. However, NVSS is less deep than FIRST and consequently the matched sample contains fewer galaxies. The NVSS–FIRST–SDSS matched sample therefore does not benefit from such good statistics.

We used the Unified Radio Catalogue constructed by Kimball & Ivezić (2008) (see sample 'C' in their table 8), selecting sources which are detected by both FIRST and NVSS, and matched to within 25 arcsec. This selection yields a radio flux density limited ($S_{1.4\,\mathrm{GHz}} > 2.5$ mJy) catalogue (hereafter FIRST–NVSS) containing 141 881 sources. We cross-matched these to the ∼680 056 MGS sources adopting the same 2-arcsec match criterion used in Section 3.1. Our cross-matched catalogue contains 5719 galaxies, and we denote this as the preliminary 'comparison radio' (CR) sample. Integrated flux densities as derived by Kimball & Ivezić (2008) are adopted in our analysis.

We estimated our matching criterion of 2 arcsec to be >99 per cent complete and >99 per cent efficient (eight random matches

Table 1. Radio flux density limits, $S_{\rm lim}$, of both the radio sample (FIRST–SDSS) and the candidate CR sample (FIRST–NVSS–SDSS), the number of objects in each, and the estimated completeness and efficiency.

Matched surveys	$S_{\rm lim}$ (mJy)	Objects	Completeness (per cent)	Efficiency (per cent)
FIRST–SDSS	1.0	25 931	72	>99
FIRST–NVSS–SDSS	2.5	5719	99	>95

were found when the FIRST–NVSS RA and Dec. were offset by 1°). The FIRST–NVSS catalogue used to create the CR sample is 99 per cent complete and matched with 96 per cent efficiency (see table 2 of Kimball & Ivezić 2008). We therefore estimated the CR sample to be >99 per cent complete and >95 per cent efficient (see Table 1). Five of the 5719 galaxies in the CR sample reside in the control sample derived in Section 3.1 and these were removed. 4935 of the CR sample (86 per cent) are also in the FIRST–SDSS sample.

3.3 Redshift range

In the following sections (Sections 3.3–3.8), we discuss the secondary selection criteria applied to the FIRST–SDSS sample. The CR sample follows the same path, and a summary of the final CR sample properties are presented alongside those of the final radio sample in Section 3.9.

We imposed a redshift cut of $0.02 < z < 0.18$ to ensure that the galaxy spatial structure could be well examined. For $z < 0.02$, redshift is not a reliable distance indicator. Fig. 3 shows less than 2 per cent of matched sources have redshift <0.02. The MGS magnitude limit of $r^*_{\rm petro} < 17.77$ corresponds to $L_{r^*} > 2.6 \times 10^{23}\,{\rm W\,Hz^{-1}}$ at $z = 0.18$, and our sample should be complete to this optical luminosity density.

We restricted the SDSS-derived redshift confidence (`zconfidence`) to be greater than 95 per cent, which cuts out 12 per cent of objects from the preliminary radio sample and 10 per cent of objects from the preliminary control sample. After redshift selection, 499 418 radio-quiet galaxies remained in the control sample, ∼70 per cent of the parent MGS, whilst the radio sample contained 17 024 galaxies. The average error in redshift for both samples is <0.002, and the redshift distributions of these two samples were indistinguishable at the 1 per cent level on the basis of a two-tailed Kolmogorov–Smirnov (KS) test.

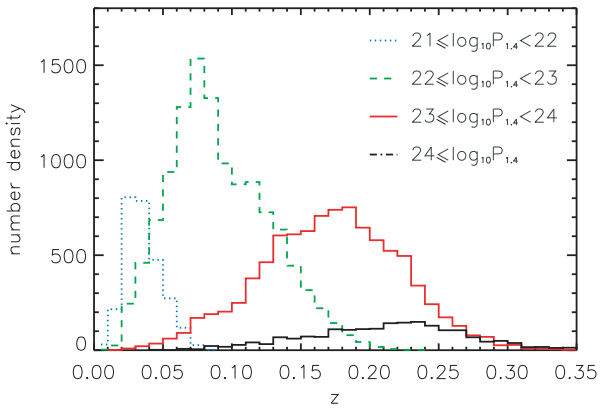

Figure 3. Distributions of FIRST–SDSS radio sample redshifts for $\log_{10}P_{1.4\,\rm GHz}$ luminosity bins. We cut at $0.02 < z < 0.18$, providing a high sample completeness (>98 per cent) down to $P_{1.4\,\rm GHz} \approx 10^{23}\,{\rm W\,Hz^{-1}}$.

3.4 Radio power

Best et al. (2005a) suggested that typical radio-loud AGN have powers above $10^{23}\,{\rm W\,Hz^{-1}}$ at 1.4 GHz, and Condon (1989) shows that $P_{1.4\,\rm GHz} = 10^{23}\,{\rm W\,Hz^{-1}}$ separates the spiral starburst population from the AGN - E/S0 population in local galaxy fields. We therefore restrict the radio sample to galaxies harbouring radio sources with $P_{1.4\,\rm GHz} > 10^{23}\,{\rm W\,Hz^{-1}}$, which selects 5119 galaxies (30 per cent) from the radio sample. Fig. 3 shows that this threshold in radio power is well matched to our redshift selection. We name this set of 5119 galaxies the 'radio-loud' sample. The mean redshift of the radio sample increased from ∼0.095 to ∼0.136 when the radio power cut was applied.

AGN can be split on the basis of large-scale radio structure into Fanaroff–Riley type I (FR I), where radio brightness decreases outwards from the centre, and FR II types, with edge-brightened lobes and hotspots (Fanaroff & Riley 1974). FR IIs are more luminous, $P_{178\,\rm MHz} \geq 1.3 \times 10^{26}\,{\rm W\,Hz^{-1}}$, and are rare in a low-redshift sample such as ours (Fig. 3), since this 178-MHz power corresponds to $P_{1.4\,\rm GHz} \approx 3.1 \times 10^{25}\,{\rm W\,Hz^{-1}}$ for a typical spectral index of $\alpha = 0.7$.

3.5 Removing type 1 AGN

In unified AGN models (e.g. Antonucci 1993), the appearance of the central black hole and associated continuum of an AGN differ only in the viewing angle at which it is observed. Sources viewed face-on (type 1) show broad emission lines that are absent in those observed edge-on and where the broad emission line region is obscured by a dusty torus (type 2). Type 1 AGN are excluded from this study, as the optical continuum can be dominated by relativistically boosted non-thermal emission, which may overwhelm measurements of the host galaxy's properties.

The SDSS spectral classification pipeline automatically flags and excludes quasars from the MGS, but we chose to verify its reliability and the relative numbers of type 1 AGN remaining in our sample. We followed the method outlined by Masci et al. (2010) to identify broad-line emission. Hα or Hβ emission lines exceeding $1000\,{\rm km\,s^{-1}}$ (FWHM) with a signal-to-noise ratio S/N > 3 and Hα/Hβ equivalent width EW > 5 Å were classified as broad line. Galaxies with both broad Hα and Hβ emission were classified as type 1 AGN. Three galaxies of the 5119 radio-loud sample have broad Hα and Hβ emission lines and were removed from the sample.

184 galaxies (4 per cent) of the remaining 5116 radio-loud sample have broad Hα emission, but do not have broad Hβ emission.

Osterbrock (1989) classified these objects as type '1.9' AGN, which have substantial but not complete obscuration of the central continuum source. Kauffmann et al. (2003) determine that the contribution to the observed continuum is not significant in these sources, so we retain these within our sample. The control sample contained 10 type 1 AGN and 1835 type '1.9' AGN. We removed the type 1 AGN to leave 499 408 galaxies within the control sample.

3.6 Removing star-forming galaxies

Type 2 AGN have narrow permitted and forbidden lines and their stellar continuum is often similar to normal star-forming galaxies (SFGs). Yun, Reddy & Condon (2001) show a tight correlation between far-IR luminosity (indicative of SF) and $P_{1.4\,\rm GHz}$. This will cause a level of contamination by SFGs if $P_{1.4\,\rm GHz}$ is used as the sole tracer of galaxies hosting a radio-loud AGN. We should therefore

remove the small subset of radio-loud galaxies in which the radio power arises from SF and not from an AGN.

AGN separation from SF galaxies in the local Universe can be achieved via optical emission line ratio diagnostics (Baldwin, Phillips & Terlevich 1981, hereafter BPT). Emission-line ratios probe the ionizing source: for AGN, non-thermal continuum from the accretion disc around a black hole and in SFGs, photoionization via hot massive stars. However, Best et al. (2005b) find no correlation between a galaxy being radio-loud and whether it is optically classified as an AGN. In agreement with this, we found no correlation[3] between radio flux at 1.4 GHz and the optical line ratios [N II]/Hα or [O III]/Hβ in our sample. Hence, a substantial fraction of radio-loud AGN would not be selected using BPT diagnostics, and were we to apply them to the radio sample it would be biased towards radio galaxies with particularly strong optical emission lines.

We instead remove galaxies which are strongly identified as non-AGN, i.e. star forming. Despite this method leaving a small fraction of SFGs which are faint in optical line emission, all radio-loud AGN, whether optically bright or otherwise, will remain in the sample. This decrease in efficiency of the sample is preferential to a drastic decrease in completeness. A similar problem was identified by Sadler et al. (2002), who defined a sample of radio-loud AGN from the 2dFGRS catalogue. They found approximately half of the sample have absorption spectra similar to those of inactive giant ellipticals, and therefore would be mostly missed by optical AGN emission-line selection.

In classifying galaxies as AGN or star forming, we utilized the demarcation criterion of Kauffmann et al. (2003):

$$\log([\mathrm{O\,III}]/\mathrm{H}\beta) > 0.61/\{\log([\mathrm{N\,II}]/\mathrm{H}\alpha) - 0.05\} + 1.3, \quad (2)$$

plotted as the dashed line on Fig. 4.

Fig. 4 shows the standard line ratio diagnostics for galaxies from the radio-loud sample with all four emission lines catalogued in the SDSS (grey crosses, 1069 objects of the 5116). 766 of these 1069 galaxies have both optical emission-line ratios at S/N $\geq$ 3 and their density on the BPT diagram is shown as contours. 118 (11 per cent) lie below the demarcation line and are marked with red circles (112 out of these 118 have all four emission lines with S/N $\geq$ 5). We removed these 118 optically selected SF galaxies from the radio-loud sample, to leave a sample of 4998 predominantly radio-loud AGN hosts.

We then estimated the residual contamination expected in the radio AGN sample from SFGs by plotting the maximum uncertainty for a point on the Kauffmann separator with S/N of 3 (Fig 4, dotted lines). 69 objects detected at S/N >3 (black crosses) lie between the Kauffmann separator and the upper maximum uncertainty line. Therefore, the contamination expected in the radio AGN sample from SFGs is $\sim$11 per cent.

Our radio sample contains predominantly FR I galaxies, which are usually hosted by giant elliptical galaxies and on average have weak or no optical nuclear emission lines (Lin et al. 2010, and references therein). Within our sample of radio-loud AGN, 79 per cent of objects do not have optical emission line fluxes. We estimate $\approx$11 per cent contamination of non-AGN (e.g. SFG) if galaxies without SDSS emission lines are similar to galaxies with bright line emission. Five galaxies without emission line fluxes >3σ lie below the demarcation line in Fig. 4 and are potentially star forming, but without reliable line information we retain these within our sample.

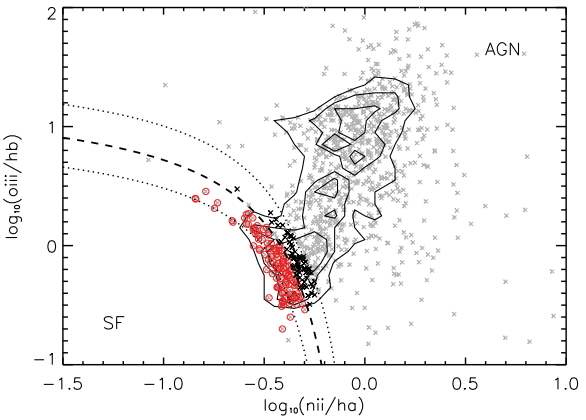

Figure 4. BPT diagram for galaxies within the radio-loud sample with emission line ratios. 1069 galaxies from the 5116 radio-loud sample have emission line ratios and are plotted as grey crosses where the size of the symbol does not indicate the sizes of the error bars, which vary widely. The dashed curve (equation 2) indicates the demarcation given by Kauffmann et al. (2003) between optical AGN (above the line) and SF galaxies (below the line). 766 galaxies plotted have emission-line ratios with >3σ significance. The density of these galaxies is shown by contours, 85 per cent of the 766 galaxies lie above the line as optically classified AGN. The remaining 15 per cent (118 galaxies) lie below the curve (red circles) and we classified these as star forming. We also show the maximum uncertainty for a point on the Kauffmann separator with S/N of 3 (dotted lines). 69 objects detected at S/N >3 (black crosses) lie between the Kauffmann separator and the upper maximum uncertainty line.

As discussed by Best et al. (2005b), a potential shortfall of spectral classification of emission-line radio-loud AGN is that emission-line AGN activity is often accompanied by SF (e.g. Kauffmann et al. 2003). This SF will give rise to radio emission, even if the AGN itself is radio-quiet. For these sources, the optical spectrum could still be dominated by a (radio-quiet) AGN leading to classification as an emission-line radio-loud AGN.

Morić et al. (2010, hereafter M10) derive a population of sources matched from all NVSS galaxies in the Unified Radio Catalogue (Kimball & Ivezić 2008), the SDSS-MGS and *IRAS* data. The matched sources are divided into star forming, composite and AGN using standard BPT diagnostics. SF rates are derived via broad-band spectral fitting to the near-UV–near-IR SDSS photometry, and the *average* fractional SF/AGN contribution to the radio power is estimated (see their table 2). They find that in 203 composite galaxies, 81.3 per cent of the total radio power is due to SF. The variation of this fraction with radio power is not specified.

Following M10, we defined 206 composite galaxies in our own radio sample (27 per cent of the emission-line galaxies confirmed at S/N $\geq$ 3), using the diagnostics of Kewley et al. (2001) and Kauffmann et al. (2003). If the average fractional contribution is independent of total radio luminosity, then we estimated an upper limit of $\sim$27 per cent of our radio sample may have radio power boosted by SF but possess a radio-quiet AGN. However, $\lesssim$14 per cent of the composite sample defined by M10 have $\log[P_{1.4}(\mathrm{W\,Hz^{-1}})]$ >23. Mauch & Sadler (2007) find SF galaxies tend to have median $\log[P_{1.4}(\mathrm{W\,Hz^{-1}})] = 22.13$, whereas AGN have a median $\log[P_{1.4}(\mathrm{W\,Hz^{-1}})] = 23.04$. Therefore, our luminosity cut will have significantly reduced the numbers of galaxies where SF is the principal contributor to the total radio power, and we expect far less than 27 per cent contamination from radio-quiet, optically loud AGN.

[3] Spearman's rank correlation result is $\pm$0.06 or less between the radio flux and optical emission-line flux ratios for our radio galaxy sample.

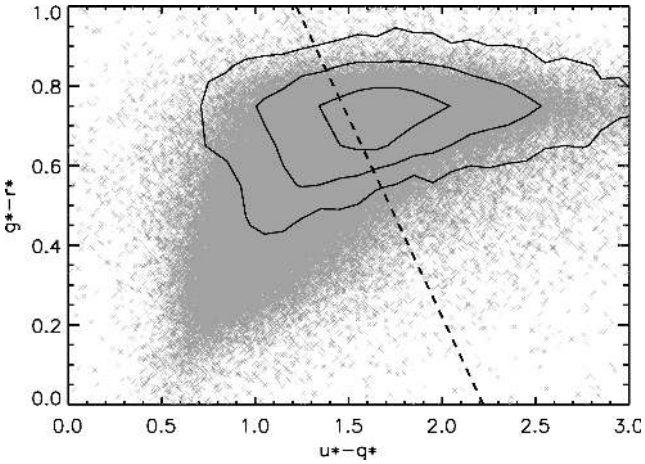

Figure 5. Colour–colour plot for the entire control sample (grey) and 34606 visually classified ellipticals from Galaxy Zoo–control sample match ($\log_{10}$ contours). The dashed line is $u^* - r^* \geq 2.22$ mag from Strateva et al. (2001) and defines a morphological colour separator. 80 per cent of the Galaxy Zoo–MGS sample lie above the line. The u^*, g^* and r^* mag are derived from SDSS columns: `petrocounts − reddening − kcorr`.

We also cannot account for the population of 'composite' radio-loud host galaxies with ongoing SF that have been lost from our sample through this selection technique. Mauch & Sadler (2007) estimate that ∼10 per cent of local radio sources may have a star-forming spectrum, but have radio flux densities dominated by a radio-loud AGN.

3.7 Colour bimodality

As low-redshift radio-loud AGN are hosted predominantly by elliptical galaxies, we attempted to constrain the control sample to contain only early-type galaxies. The colour distributions of galaxies have been shown to be highly bimodal (Yan et al. 2006, 2011; Strateva, Ivezić & Knapp 2001). Fig. 5 shows a colour–colour plot in $g^* - r^*$ against $u^* - g^*$ as explored by Strateva et al. (2001) who define an optimal colour separator[4] between early and late types of $u^* - r^* \geq 2.22$ mag. Early types (E, S0, Sa) populate the upper right region, and late types (Sb, Sc, Irr) occupy the lower left.

In order to test the completeness of this demarcation, we used the 62 190 galaxies visually classified as ellipticals in Galaxy Zoo data (Lintott et al. 2011). We cross-matched these to the control sample, selecting objects within 1-arcsec radius. 34 606 matches were found, and 27 569 of these lie above $u^* - r^* > 2.22$ mag. Therefore, this demarcation gives ∼80 per cent reliability (Fig 5, contours), suggesting ∼20 per cent of the early-type galaxy population may be excluded through applying this criterion. 147 275 visually classified 'spiral' galaxies from the Galaxy Zoo data are also present in our control sample. 22 per cent of these lie above $u^* - r^* > 2.22$, i.e. we expect ∼22 per cent contamination in the early-type sample. Of the 499 408 galaxies in the control sample, ∼40 per cent were classified as early types, using the Strateva et al. colour selection, to leave 199 391 early-type galaxies in the control sample, morphologically selected in colour space at ∼80 per cent completeness and ∼78 per cent efficiency based on Galaxy Zoo visual analysis.

[4] On a spectroscopically classified galaxy sample, early types are recovered at $\gtrsim$98 per cent completeness and $\gtrsim$83 per cent reliability.

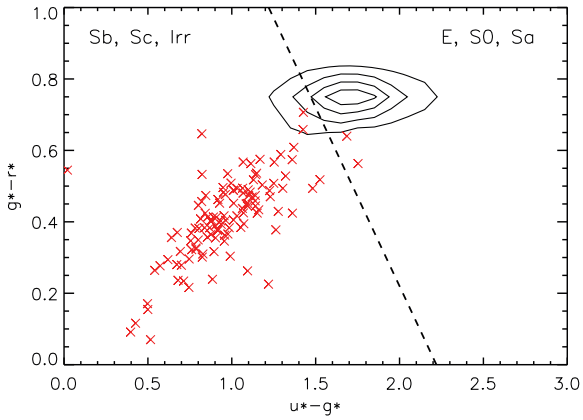

Figure 6. Colour–colour plot of radio-loud AGN (contoured, bin size = 0.1×0.1 mag, four equally spaced levels, max density contour = 400 bin^{-1}), and SF galaxies as defined in Section 3.6 (crosses). The dashed line is $u^* - r^* \geq 2.22$ from Strateva et al. (2001) and defines a morphological colour separator.

We explore the 4998 radio-loud AGN-selected galaxies in colour space. Fig. 6 shows the radio-loud AGN are predominately early types, with >70 per cent lying above $u^* - r^* > 2.22$, i.e. the radio-loud AGN sources are predominantly hosted by ellipticals as defined in colour space. The distribution in colour space is similar to that of the control sample, despite the AGN colours possibly influencing the light. In agreement with this result, Griffith & Stern (2010) found radio-selected AGN have a high incidence of being hosted by early-type galaxies.

The 118 galaxies we flagged as star forming and removed from the radio-loud sample in Section 3.6 are shown as crosses in Fig. 6, and 98 per cent of these sit below the line. We select the radio-loud AGN above the colour cut, to give 3516 'early-type' radio-loud AGN hosts.

3.8 Redshift distributions

At this stage we re-examined the redshift distributions of the samples, using the KS test. The probability of the control sample and the radio-loud AGN being drawn from the same parent sample in redshift was <0.1 per cent: the distributions in redshift differ (Fig. 7a). Evolutionary differences in host galaxy properties should be small over this entire redshift range, however we chose to resample the control sample redshift distribution to match that of the radio-loud AGN sample.

We also examined the intrinsic r^*-band luminosity of the two samples. Fig. 7(b) shows the radio sample is globally brighter in r^* than the control sample. It has been well established that radio-loud AGN are hosted preferentially in the brightest and most massive elliptical galaxies (Best et al. 2005b; Mauch & Sadler 2007). Since we wanted to test whether radio-loud AGN harbour an excess of blue emission in their centres, we chose to resample the control sample to have the same r^*-band optical properties so as to avoid any possible correlation of colour gradient with galaxy luminosity.

We generated a matched control sample by selecting the 10 galaxies from the whole sample that lie closest to each radio-loud AGN in magnitude–redshift space. The final control sample contains 35 160 galaxies, whose magnitude and redshift distributions are shown as dotted lines in Fig. 7. This final selection should allow the distribution of observables in the radio and control samples to be compared directly.

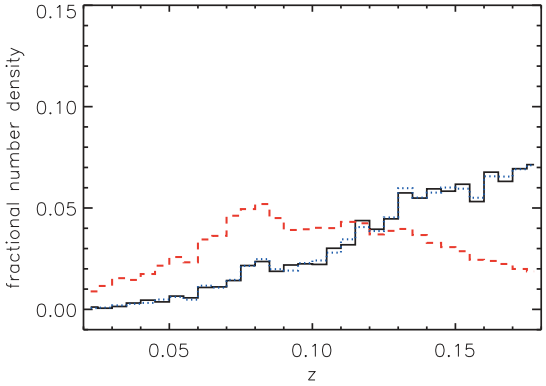

(a) Redshift distributions

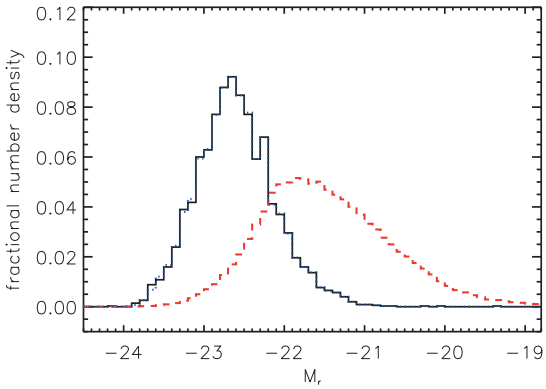

(b) Absolute r^* magnitude distributions

Figure 7. The fractional distributions of (a) redshift and (b) r^*-band luminosity. The solid black line shows the radio-loud AGN distributions. The red dashed line shows the control sample distribution prior to nearest neighbour matching in redshift–magnitude space. The blue dotted line shows the resultant sample randomly selected to match the redshift–magnitude distributions of the radio sample.

3.9 Comparison radio sample

The criteria applied to the 'radio' sample in Section 3.3–3.8 were also applied to the 5719 objects in the CR sample (see Section 3.2).

We imposed a redshift cut of $0.02 < z < 0.18$ and restricted the redshift confidence parameter given by SDSS to >95 per cent, leaving 3727 sources. We examined the CR sample radio powers based on NVSS and FIRST. Fig. 8 shows the NVSS and FIRST luminosities for the 3727 CR sources (grey crosses). Those with $P^{\rm NVSS}_{1.4\,\rm GHz} > 10^{23}\,\rm W\,Hz^{-1}$ are highlighted by blue squares (50 per cent). We restricted the CR sample to galaxies harbouring radio sources with $P^{\rm NVSS}_{1.4\,\rm GHz} > 10^{23}\,\rm W\,Hz^{-1}$, which selects 1847 (50 per cent) of the sample.

Of those 1847 sources, 251 have FIRST-derived powers $<10^{23}\,\rm W\,Hz^{-1}$, and were therefore excluded in the radio sample selection in Section 3.4.

We removed two type 1 AGN and 48 SFGs confirmed at S/N > 3 from the CR sample, leaving 1797 radio-loud narrow-line AGN hosts. 4 per cent of the sample are classified as type '1.9' AGN, with substantial but not full obscuration of the central source. We applied the Strateva et al. colour cut ($u^* - r^* > 2.22$ mag) detailed in Section 3.7, to select 1295 early-type galaxies from the CR sample.

The control sample was cross-matched with the FIRST–NVSS catalogue to within 2 arcsec, and the five galaxies found were removed to ensure the comparison control sample is comprised solely of 'radio-quiet' AGN elliptical hosts. 199 386 galaxies remain in the CR–control sample.

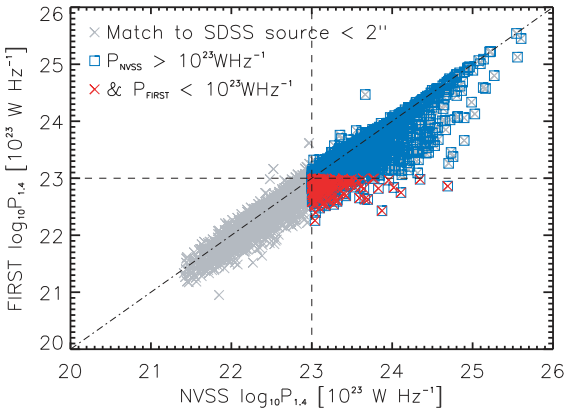

Figure 8. FIRST versus NVSS derived luminosities for the 3737 sources in the candidate CR sample (grey crosses). Those with $P^{\rm NVSS}_{1.4\,\rm GHz} > 10^{23}\,\rm W\,Hz^{-1}$ are highlighted by blue squares (1847). Of those, 251 sources with $P^{\rm FIRST}_{1.4\,\rm GHz} < 10^{23}\,\rm W\,Hz^{-1}$ are shown as red crosses. These are the sources excluded in the radio sample's luminosity cut (Section 3.4).

We selected the 10 galaxies from the control sample that lie closest to each CR radio-loud AGN in magnitude–redshift space. The final CR–control sample contains 12 950 sources, matched to the CR sample in r^*-band magnitude and redshift distributions.

3.10 Summary of final samples

3.10.1 Radio-loud 'early-type' AGN (R-AGN) – 3516 sources

After matching FIRST to the MGS ($r^*_{\rm petro} < 17.77$ mag, $0.02 < z < 0.18$) within 2 arcsec, we classified as radio-loud AGN hosts with $P_{1.4\,\rm GHz} > 10^{23}\,\rm W\,Hz^{-1}$. Type 1 AGN exhibiting both broad Hα and Hβ emission lines were removed from the sample. Optical emission-line ratios (if confirmed at 3σ) were used to remove SFGs using the demarcation of Kauffmann et al. (2003). We then created a subset with $u^* - r^* > 2.22$ mag, i.e. 'early types' to remain consistent with the colour cut applied to the control sample.

3.10.2 Control sample – 35160

We removed all galaxies from SDSS-MGS ($r^*_{\rm petro} < 17.77$ mag, $0.02 < z < 0.18$) with FIRST and NVSS counterparts. Type 1 AGN exhibiting both broad Hα and Hβ emission lines were removed from the sample. Galaxies were constrained in colour to bias towards early-type morphology where a comparison with results of the Galaxy Zoo program suggests we have $\gtrsim 80$ per cent completeness and 78 per cent efficiency. The resultant sample comprises radio-quiet, 'normal', predominantly elliptical galaxies.We then selected a subsample to match the redshift and optical r^*-band magnitude distributions of the R-AGN sample, thus removing any redshift bias and potential correlation of colour gradient with galaxy luminosity.

3.10.3 Comparison radio (CR) – 1295 sources

We cross-matched the FIRST–NVSS catalogue derived by Kimball & Ivezić (2008) with the MGS ($r^*_{\rm petro} < 17.77$ mag, $0.02 < z < 0.18$) to within 2 arcsec, and classified radio-loud AGN hosts as those

sources exhibiting $P_{1.4\,\mathrm{GHz}}^{\mathrm{NVSS}} > 10^{23}\,\mathrm{W\,Hz^{-1}}$. Type 1 AGN exhibiting both broad Hα and Hβ emission lines were removed from the sample. Optical emission-line ratios (if confirmed at 3σ) were used to remove SFGs using the demarcation of Kauffmann et al. (2003). We then created a subset with $u^* - r^* > 2.22$ mag, i.e. 'early types' to remain consistent with the colour cut applied to the control sample.

3.10.4 CR–control sample – 12950 sources

All selection criteria as above for the control sample, we also removed five galaxies within the control sample that were also present in the CR sample. We then selected a subsample to match the redshift and optical r^*-band magnitude distributions of the CR sample.

We therefore have two radio-loud AGN samples, both with a comparison control sample. The CR sample is derived using both radio catalogues, and is a brighter radio sample (the NVSS flux density completeness limit is 2.5 mJy) for comparison with our deeper (>1 mJy), larger, but more incomplete, R-AGN sample derived solely from the FIRST catalogue.

4 ANALYSIS

The surface brightness profile of an early-type galaxy can be described by the Sérsic equation:

$$I(r) = I(r_\mathrm{e})\mathrm{e}^{-b[(r/r_\mathrm{e})^{1/n}-1]}, \quad (3)$$

where r_e is the effective radius (scalelength) and $I(r_\mathrm{e})$ is the corresponding effective surface brightness. $b \approx 2n - 1/3$ is chosen so r_e contains half the light in the galaxy. $n \approx 4$ for bright ellipticals decreasing to $n \approx 2$ as luminosity decreases (Caon, Capaccioli & D'Onofrio 1993). SDSS chooses to fix $n = 4$, fitting the 'de Vaucouleurs profile', truncating the profile beyond $7\,r_\mathrm{e}$. The model fitted by SDSS has an arbitrary axial ratio and position angle and is convolved with a double-Gaussian representation of the point spread function. The fitting then yields, among other properties, the effective radius, r_e, and error, Δr_e. In general, the error for the u model is greater than other bands. It is noted that SDSS's fitting algorithm generates some weak discretization of model parameters, especially in $r_\mathrm{e}(r)$ and $r_\mathrm{e}(u)$. Objects with scalelengths lying in discrete bands in r_e tend to have poorer goodness of fit. This is not included in the error estimates, Δr_e, which were derived from count statistics on the image. In our work with the r_e values, we consider Δr_e rather than `DeV_l` (the likelihood of the model fit) due to our reluctance to remove data with poor de Vaucouleurs u-band fitting. A poor goodness of fit to the de Vaucouleurs profile may be indicative of a cuspy u band, and removing such objects could bias results.

SDSS denotes the `fracDeV` parameter as the fraction of the total flux contributed by the de Vaucouleurs component in a linear combination of a de Vaucouleurs and an exponential model to find the best fit. It is noted that the likelihood values in the r^* band are intrinsically poor (all samples have mean values ∼0.01), but the likelihood ratios still pick out reliable best-fitting parameters. The `fracDeV` parameter (f hereafter) is correlated with the Sérsic index; $n = 1$ corresponds to $f = 0$, $n = 4$ corresponds to $f = 1$ (see Kuehn & Ryden 2005, and references therein). Following Vincent & Ryden (2005), galaxies with $0.5 \leq f \leq 0.9$ ($2.0 \lesssim n \lesssim 3.3$) are labelled 'de/ex' galaxies and galaxies with $f \geq 0.9$ ($n \gtrsim 3.3$) are labelled 'de' galaxies. We chose not to remove objects with $f < 0.5$, but instead created subsets of each sample with $f > 0.5$ for comparison.

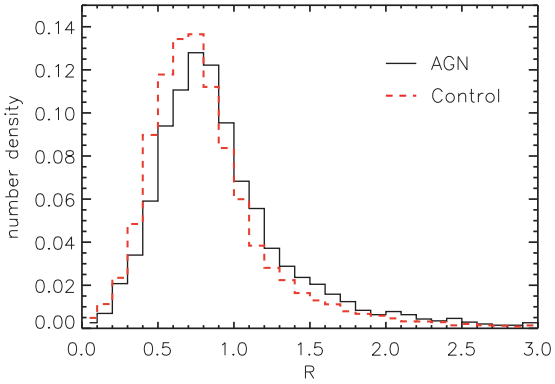

Figure 9. Normalized distributions of R for the R-AGN sample (solid) and the control sample (red dashed).

We investigate the colour structure of AGN host galaxies principally through the distribution of R, which we define as $R = r_\mathrm{e}(r)/r_\mathrm{e}(u)$, which is the ratio of r to u de Vaucouleurs effective radii. This should avoid any intrinsic scale differences in r and u between individual galaxies.

4.1 Diversity of intrinsic distributions

The distributions of R for the R-AGN and control sample are shown in Fig. 9. Both samples have a few (<0.001 per cent) strong outliers ($R > 100$) which significantly disturb the mean. The medians of the R-AGN and control distributions are 0.837 and 0.793, respectively. Using a two-tailed KS test, we find the probability of the control and the R-AGN samples being drawn from the same distribution to be small (<0.1 per cent).

Similarly, the CR sample's R distribution also shows a higher median compared to the CR–control sample (0.851 and 0.797, respectively). The KS test also finds the probability of the CR and CR–control sample being drawn from the same distribution in R is vanishingly small (<0.1 per cent).

4.2 Maximum likelihood analysis

The fractional errors in individual values of $r_\mathrm{e}(u)$ are relatively large, which makes proving an intrinsic difference between the radio-loud AGN samples and their respective control sample distributions challenging. We used a maximum likelihood analysis to compare the average values of R for the AGN and control samples, taking into account measurement errors according to Maccacaro et al. (1988) and Worrall (1989), in order to quantify the difference between the distributions of R.

Under the assumption that both the AGN and control samples have normally distributed intrinsic values of R, then the population mean, $\overline{R}$, and intrinsic dispersion, σ, of either can be determined from individual values $R_i \pm \sigma_i$ by minimizing the function:

$$S = \sum_i \left[\frac{(R_i - \overline{R})^2}{(\sigma^2 + \sigma_i^2)} + \ln(\sigma^2 + \sigma_i^2) \right]. \quad (4)$$

Fig. 10 shows the results of minimization of equation (4) across $\overline{R}$ and σ parameter space, for the two samples. The 90 and 99 per cent joint-confidence contours for $\overline{R}$ and σ are given by $S_\mathrm{min} + \Delta S$ for $\Delta S = 4.61$ and 9.21, respectively. Table 2 shows the best-fitting $\overline{R}$ and σ planes for both distributions. A clear separation between radio-loud 'early-type' AGN and 'normal' control galaxies can be

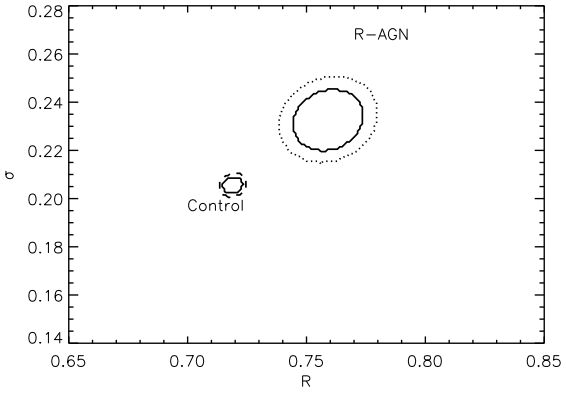

(a) R-AGN and control

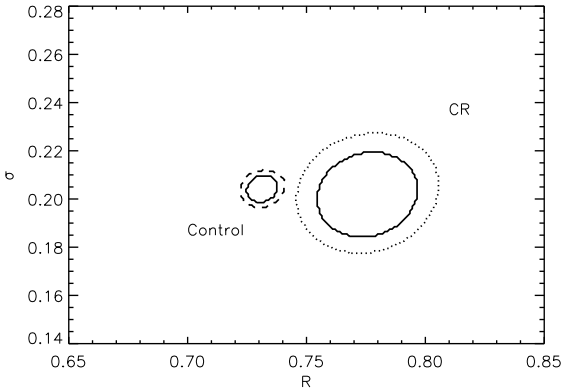

(b) CR and CR-control

Figure 10. 90 per cent (solid line) and 99 per cent (dashed/dotted line) confidence contours of the mean ratio of scalelengths [$R = r_e(r)/r_e(u)$] and intrinsic dispersion for radio-loud AGN galaxies and 'normal' early types. The control and radio-loud 'early-type' AGN are distinct populations, as are the CR and CR–control samples.

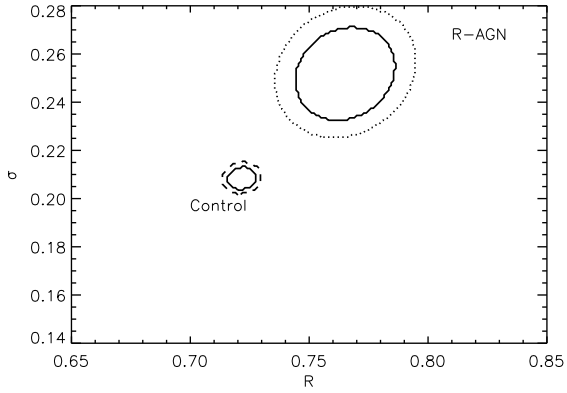

(a) R-AGN and control

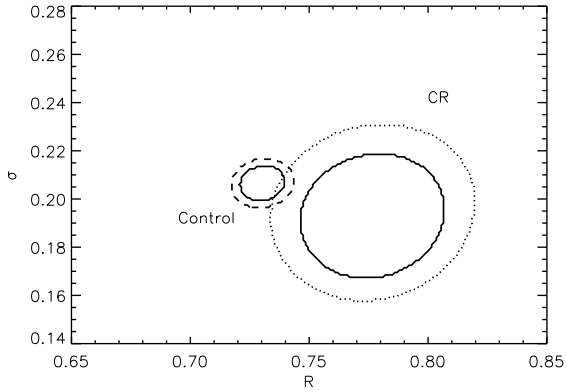

(b) CR and CR-control

Figure 11. 90 per cent (solid line) and 99 per cent (dashed/dotted line) confidence contours of the mean ratio of scalelengths [$R = r_e(r)/r_e(u)$] and intrinsic dispersion for the subset of galaxies with $f > 0.5$. The 1851 radio-loud AGN galaxies and 17 338 'normal' early types are shown in panel (a), the 575 CR galaxies and 6364 CR–control galaxies are shown in panel (b). The control and radio-loud 'early-type' AGN remain distinct populations. The smaller CR and CR–control sample lead to larger confidence contours that overlap, but these remain distinct at 89 per cent confidence.

seen for both the R-AGN and CR samples, and we conclude the two are not drawn from the same population at $\gg$99 per cent confidence.

We applied the cut $f > 0.5$ in the r^* band, and re-examine the results for both radio-AGN samples. This cut will ensure the reliability of the de Vaucouleur's scalelengths used to derive R, and this subset is used as a comparison to the full samples to verify whether galaxies with shapes that differ significantly from the de Vaucouleurs profile perturb our main result. Table 2 also shows the fraction of each sample with 'good' de Vaucouleurs r^*-band fits and their $\overline{R}$ values (see Fig. 11). Although the values do not significantly differ from the full sample, the confidence contours now overlap in the smaller, but more complete, CR sample. However, the R-AGN and control samples are still seen to come from distinct populations.

5 DISCUSSION

Our results confirm that radio-loud AGN are hosted by brighter, bigger galaxies on average (see Fig. 7). Our technique has shown the presence of an AGN is associated with an increase of the scale size of a galaxy in red light relative to blue light. This suggests that radio galaxies have a bluer central bulge and/or more diffusely

Table 2. Best-fitting $\overline{R}$ and σ corresponding to 90 per cent error, for the R-AGN and CR samples, and their relative control samples. The fraction of each sample with r^*-band $f > 0.5$ is shown, and the resultant mean and standard deviation, $\overline{R}_f$ and σ_f.

Sample	$\overline{R}$	σ	$f > 0.5$	$\overline{R}_f$	σ_f
R-AGN	0.76 ± 0.02	0.23 ± 0.01	53 per cent	0.77 ± 0.02	0.25 ± 0.02
Control	0.719 ± 0.005	0.206 ± 0.003	49 per cent	0.722 ± 0.006	0.208 ± 0.005
CR	0.78 ± 0.02	0.20 ± 0.02	44 per cent	0.77 ± 0.03	0.19 ± 0.03
CR–control	0.731 ± 0.007	0.204 ± 0.006	49 per cent	0.730 ± 0.010	0.206 ± 0.007

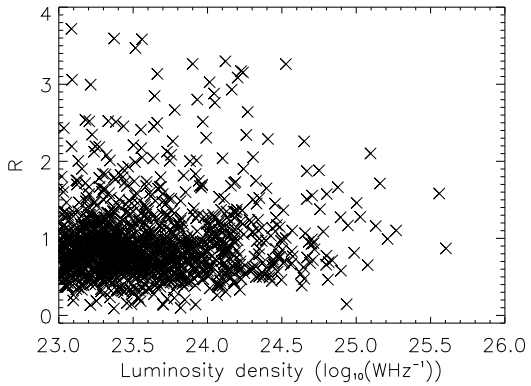

Figure 12. Radio luminosity density versus R for the CR sample. We found no correlation (>99 per cent certainty) between the two.

distributed red light compared to their radio-quiet counterparts. With the analysis so far, we cannot tell whether this difference is from AGN-driven or diffuse star-like light within the bulge or more distributed red light.

The CR sample is also significantly different in $\overline{R}$ relative to the CR–control sample, so that our R-AGN sample's lower completeness in extended sources does not significantly affect the result. The CR sample dispersion is smaller than that of the R-AGN sample, whereas all four control samples have values of σ that are similar. We applied a flux cut of >4 mJy to the R-AGN sample (61 per cent), and found $\overline{R} = 0.80 \pm 0.02$ and $\sigma = 0.21 \pm 0.01$. The increased scatter about R is caused by fainter radio sources, which tend to be more heterogeneous, and/or have underestimates of errors on r_e values in more distant objects.

The subset of CR galaxies constrained to have good r^*-band de Vaucouleurs fits ($f > 0.5$) does not contain enough radio galaxies to show strongly a significant separation from the CR–control sample [see Fig. 11(b)]. We present discussion predominantly on the R-AGN and control sample, which display a clear separation in both Figs 10(a) and 11(a). We concluded the two are not drawn from the same population at $\gg$99 per cent confidence. This sample is incomplete to radio sources with lobes >5.4 arcsec and the population of galaxies with a weak radio AGN core but powerful lobes. However, it is large due to the depth of the FIRST survey. The CR results for all figures in the discussion are similar to the results presented for the R-AGN sample. We find no significant deviation between the two in any subsequent parameter examined, except in σ, as discussed above.

Mahabal et al. (1999, hereafter MKM99) used a complementary ratio[5] to demonstrate the ubiquity of inner blue components in a sample of only 30 radio galaxies and 30 control galaxies, and argued that the blue light is due to SF associated with the presence of a radio source (e.g. Antón, Browne & Marchã 2008). Fig. 4 of MKM99 (power at 408 MHz versus log $[r_e(B)/r_e(R)]$) shows a trend for more powerful radio galaxies to have steeper colour gradients as indicated by the ratio of scalelengths. In contrast to this, when considering only the brightest ($P_{1.4\,\mathrm{GHz}} > 10^{25}\,\mathrm{W\,Hz^{-1}}$) radio sources in the CR sample (for which the powers are more accurate), we find no correlation between radio power and R. We also find no correlation over the full range of radio powers and R as shown in Fig. 12: the Spearman's rank correlation result is ± 0.07 or less between $P_{1.4\,\mathrm{GHz}}$ and R. We infer that a high value of R (and possible blue central bulge) is not associated with the power of the radio source.

There are several possible scenarios to be considered to explain the larger R in the R-AGN sample.

5.1 AGN light

Central point-like u^* light may be indicative of a blue AGN. We investigated the nature of the R-AGN excess R, using the goodness of the de Vaucouleurs fit. The SDSS de Vaucouleurs fitting procedure returns the likelihood (between 0 and 1) associated with the model from the χ^2 fit. If the u^*-band goodness of fit for the R-AGN sample approaches 1 for low R and 0 for high R, then this is indicative of an AGN/core component (as the AGN point-like component would perturb a de Vaucouleurs fit) driving a blue excess and high R. If no structure is seen in R versus de Vaucouleurs u^*-band goodness of fit in either sample, then any blue excess is more likely driven by some sort of diffuse starlight in the central bulge.

The u^*-band data for both the R-AGN and control samples are generally well fitted by a de Vaucouleurs profile (the R-AGN/control median likelihood values are 0.86 and 0.83, respectively), and there is no trend for the u^*-band or r^*-band fits to be worse at large R in the R-AGN than the control sample. We can conclude that the high R in the R-AGN sample is not due to any point-like AGN component.

5.2 Radio AGN triggering star formation

It is generally agreed that AGN feedback regulates the supply of cold gas for SF by supplying energy to the ISM and IGM. Some radio-loud star-forming AGN show a connection between the suppression of SF and the strength of the radio jets, by heating and expelling the surrounding gas (Nesvadba et al. 2008). Schawinski et al. (2009) looked at a sample of low-redshift SDSS early-type galaxies for which late-time SF is being quenched. They found that molecular gas disappears less than 100 Myr after the onset of accretion on to the central black hole. These galaxies were not associated with radio jets, but show that low-luminosity AGN episodes are sufficient to suppress residual SF in early-type galaxies.

The residual fractional number density distribution of scalelengths are shown in Fig. 13, for the control sample subtracted from the R-AGN sample. There is a clear excess of blue cores (0.1–10 kpc) in the R-AGN sample as compared to the control sample. There are also more small $r_e(r^*)$ in the R-AGN sample, ranging from 4 to 10 kpc. This plot does not demonstrate the correlation between the red and blue emission, which is shown in Fig. 14, but it does demonstrate that the presence of a radio AGN seems not to have suppressed SF in the central regions of its host galaxy. Fig. 14 plots $r_e(u^*)$ against $r_e(r^*)$ for the R-AGN sample (black) and the control sample (red dashed). The dot–dashed line denotes the locus $r_e(r^*) = 0.719 r_e(u^*)$ as defined by the control sample (see Table 2).

At $r_e(r^*) > 0.719 r_e(u^*)$, the surface brightness in u^* increases more rapidly towards the centre of a galaxy than in r^* as compared to the mean of the control sample, i.e. half the blue light from the galaxy is contained in a smaller region than half the red light, implying the galaxy becomes bluer inwards.

The distribution of number densities in Fig. 14 shows radio galaxies appear to become bluer inwards more often than the control galaxies (66 per cent of the R-AGN sample are above the locus $r_e(r) = 0.719\, r_e(u)$, compared to 60 per cent of the control sample).

[5] $r_e(B)/r_e(R)$.

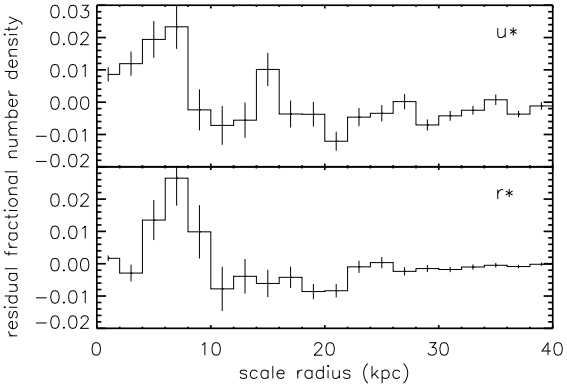

Figure 13. Residual fractional number density distributions (R-AGN–control), in 2 kpc bins, for the u^*-band and r^*-band scale radii. There is a higher fraction of blue cores in the R-AGN sample as compared to the control sample at $r_e \sim 10$ kpc. This plot does not demonstrate the correlation between the red and blue scale radii (see Fig. 14). The measurement errors are larger in the u^* band which may account for the higher variability in the residuals.

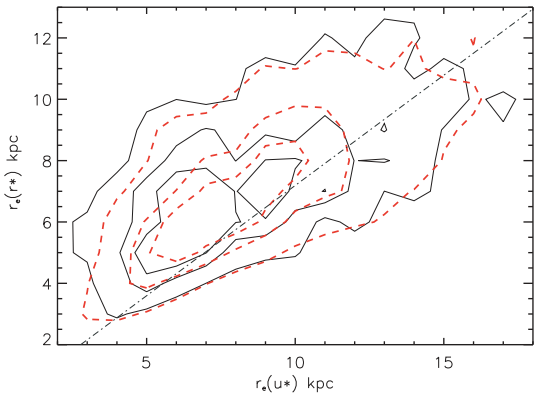

Figure 14. Normalized number densities of $r_e(u^*)$ and $r_e(r^*)$ for the R-AGN (solid) and control sample (red dashed). The dot–dashed line is the locus $r_e(r^*) = 0.719 r_e(u^*)$, galaxies above this line become bluer inwards. Contours show the fractional number densities of each sample with levels at 0.004, 0.008 and 0.011. There is a larger fraction of the R-AGN sample above the line, possibly denoting a tendency to become bluer inwards more often than the control sample.

There are fewer blue smaller cores in the control sample as compared with the R-AGN sample (see also Fig. 13), implying there may be a blue excess near the AGN core for some of the radio galaxies. However, the higher R values of the R-AGN sample also seem to be driven by a higher scalelength in r^*, seen in the difference between the inner two contour levels of each sample (see also Section 5.4), so we cannot definitively conclude that the increased R in the R-AGN sample is due to SF within the central few kpc. SF within the central few kpc would contradict feedback models which predict the suppression of SF near an AGN.

5.3 Star formation in the bulge

Shabala et al. (2008) found that radio sources in massive hosts are re-triggered more frequently than their less massive counterparts, suggesting that the onset of an AGN quiescent phase is due to fuel depletion. AGN activity is therefore promoted by an increase in gas in the centres of the galaxies, which may imply a link between the AGN radio phase and SF in the bulge (<10kpc) of the host galaxy.

It has been suggested that AGN activity and a major episode of SF in radio-loud galaxies are triggered by the accretion of gas during major mergers and/or tidal interactions. However, AGN activity is initiated later in the merger event than the starburst (e.g. Tadhunter et al. 2005; Emonts et al. 2006; Schawinski et al. 2007). Our spectroscopic selection rules out major merger events (see Section 2.1.1), but residual SF may still be present on global scales.

Observationally, there is a strong link between AGN and starbursts (Shin, Strauss & Tojeiro 2011, and references therein). Kauffmann et al. (2003) found powerful optical AGN (as classified by the strength of the [O III] emission $L_{[O\,III]} > 10^7\,L_\odot$) predominantly reside in 'young bulges'. Recent SF can provide up to 25–40 per cent of the optical/UV continuum in radio galaxies at low- and intermediate-z (e.g. Tadhunter et al. 2005; Holt et al. 2007).

We found a higher fraction of R-AGN galaxies have $r_e(u^*) <$ 10 kpc as compared to the control sample (see Fig. 13), perhaps indicative of SF in the outskirts of the bulge, fuelled by gas expelled from the central regions by the AGN.

5.4 Diffuse red emission

An alternative interpretation of a larger R is that the R-AGN sample has more distributed red light. Radio-loud 'early-type' galaxies predominantly reside in elliptical galaxies, which are well known to be redder than late types (e.g. Strateva et al. 2001). Diffuse red emission would cause a larger de Vaucouleurs scale radius in the r^* band and an increased R.

Fig. 14 suggests the increased R in the R-AGN sample may also be attributed to more diffuse red light; between $r_e(u^*) \sim 4$ and 10 kpc, $r_e(r^*)$ is on average higher for the radio population. This is also seen in the lower panel of Fig. 13.

Our results show a difference in the distributions of red and blue light in R-AGN and normal 'early-type' galaxy populations, though a high value of R is not a property of every active galaxy. We found the higher R in the R-AGN sample is contributed to by a higher fraction of radio galaxies harbouring small blue cores but also an increase in the numbers of radio galaxies with more diffuse red light as compared to the control sample. Given that SF proceeds over a longer time-scale than radio activity, this disfavours the idea that all galaxies undergo short bursts of radio activity, but rather implies that a subset has the predisposition to become radio-loud.

6 CONCLUSION

We cross-matched low-redshift ($0.02 < z < 0.18$) data from the SDSS, MGS ($r^*_{petro} < 17.77$ mag) and FIRST to within 2 arcsec, deriving a radio sample of galaxies at >99 per cent efficiency and >72 per cent completeness. Radio luminosities were in the range 10^{23}–10^{25} W Hz^{-1}. Type 1 AGN were removed from the sample (identified via Hα and Hβ broad-line characteristics), 4 per cent of the sample are classified as type '1.9' AGN, with substantial but not full obscuration of the central source. Contamination from SFGs (identified via optical emission-line ratios) in the radio sample is expected at ∼11 per cent. A control sample was defined from SDSS sources with no match to a FIRST source within 2 arcsec of their optical core, providing a sample of >99 per cent efficiency and >92 per cent completeness. At 80 per cent reliability, the demarcation $u^* - r^* > 2.22$ mag selected 'early-type' galaxies in both samples. Samples were matched in r^*-band magnitude and redshift distributions, and final sample sizes were 3516 R-AGN and 35 160 control galaxies.

We also created a complementary flux-limited sample through cross-matching with NVSS (the CR sample). The same cuts were applied to derive a radio-loud 'early-type' AGN sample, except we used the more all-encompassing NVSS flux estimates to cut in radio luminosity, thereby retaining the populations of galaxies with weak/no core radio emission but bright, extended radio lobes. This sample had higher completeness for comparison with the R-AGN sample. A control sample was defined from the SDSS sources with no match to a NVSS–FIRST source within 2 arcsec of their optical cores. We further considered only sources where `fracDeV` (f) >0.5 to restrict all four samples to having good r^*-band de Vaucouleurs fits.

We investigated the colour structure of AGN host galaxies through R, the ratio of r^* to u^* de Vaucouleurs effective radii and used maximum likelihood analysis to quantify the degree of difference in the distribution of R between samples. We concluded the radio (R-AGN/CR) samples are not drawn from the same population as their radio-faint control samples at $\gg$99 per cent confidence: the presence of an AGN increases the scale size of a galaxy in red light relative to blue light, on average.

Our result does not appear to be driven by the presence of blue AGN in the radio-loud samples since the goodness of the de Vaucouleurs fits does not become worse as R increases. We found no structure in R versus u^*-band goodness of fit in either radio sample. We found an excess of blue cores in radio-loud galaxies as compared to radio-quiet, 'early-type' galaxies, implying the increased R may be due to SF in the central few kpc, in contrast with feedback models which predict the suppression of SF near an AGN. Spectroscopic selection of our samples rules out major merger events, as starbursts can be triggered by the accretion of gas/tidal interactions. We also found radio AGN hosts to have larger red scalelengths in relation to their blue light and note this to be a contributing factor in an increased R. We cannot definitively discern whether a small blue core or larger distribution of red light is the driving factor in this result.

Given the longer time-scale for SF than radio activity, our results imply a subset of galaxies have the predisposition to become radio-loud, rather than all galaxies undergoing bursts of radio activity at some stage in their lifetimes.

ACKNOWLEDGMENTS

EJAM gratefully acknowledges support from the UK Science and Technology Facilities Council and thanks Luke Davies and James Price for helpful comments. We thank the anonymous referee for helpful and insightful comments that have resulted in an improved analysis. In undertaking this research, we made extensive use of the TOPCAT software (Taylor 2005). Funding for the SDSS has been provided by the Alfred P. Sloan Foundation, the Participating Institutions, the National Science Foundation, the US Department of Energy, the National Aeronautics and Space Administration, the Japanese Monbukagakusho, the Max Planck Society and the Higher Education Funding Council for England. This research makes use of the NVSS and FIRST radio surveys, carried out using the National Radio Astronomy Observatory Very Large Array: NRAO is operated by Associated Universities Inc., under cooperative agreement with the National Science Foundation.

REFERENCES

Abazajian K. N. et al., 2009, ApJS, 182, 543
Antón S., Browne I. W. A., Marchã M. J., 2008, A&A, 490, 583
Antonucci R., 1993, ARA&A, 31, 473
Baldwin J. A., Phillips M. M., Terlevich R., 1981, PASP, 93, 5 (BPT)
Becker R. H., White R. L., Helfand D. J., 1995, ApJ, 450, 559
Best P. N., Kauffmann G., Heckman T. M., Ivezić Ž, 2005a, MNRAS, 362, 9
Best P. N., Kauffmann G., Heckman T. M., Brinchmann J., Charlot S., Ivezić Ž, White S. D. M., 2005b, MNRAS, 362, 25
Blanton M. R., Roweis S., 2007, AJ, 133, 734
Blanton M. R., Dalcanton J., Eisenstein D., Yanny B., Yasuda N., York D. G., 2001, AJ, 121, 2358
Caon N., Capaccioli M., D'Onofrio M., 1993, MNRAS, 265, 1013
Condon J. J., 1989, ApJ, 338, 13
Condon J. J., Cotton W. D., Greisen E. W., Yin Q. F., Perley R. A., Taylor G. B., Broderick J. J., 1998, AJ, 115, 1693
Emonts B. H. C., Morganti R., Tadhunter C. N., Holt J., Oosterloo T. A., van der Hulst J. M., Wills K. A., 2006, A&A, 454, 125
Fanaroff B. L., Riley J. M., 1974, MNRAS, 167, 31p
Fukugita M., Ichikawa T., Gunn J. E., Doi M., Shimasaku K., Schneider D. P., 1996, ApJ, 111, 1748
González Delgado R., Tadhunter C., Pérez E., 2006, Astron. Nachr., 327, 159
Gonzalez-Perez V., Castander F. J., Kauffmann G., 2011, MNRAS, 411, 1151
Graham A. W., Driver S. P., Petrosian V., Conselice C. J., Bershady M. A., Crawford S. M., Goto T., 2005, AJ, 130, 1535
Griffith R. L., Stern D., 2010, AJ, 140, 533
Hogg D., Finkbeiner D. P., Schlegel D. J., Gunn J. E., 2001, AJ, 122, 2129
Holt J., Tadhunter C. N., González Delgado R. M., Inskip K. J., Rodriguez Zaurin J., Emonts B. H. C., Morganti R., Wills K. A., 2007, MNRAS, 381, 611
Ivezić Ž. et al., 2002, AJ, 124, 2364
Kauffmann G. et al., 2003, MNRAS, 346, 1055
Kewley L. J., Dopita M. A., Sutherland R. S., Heisler C. A., Trevena J., 2001, ApJ, 556, 121
Kimball A. E., Ivezić Ž, 2008, ApJ, 136, 684
Kuehn F., Ryden B. S., 2005, ApJ, 634, 1032
Lin Y., Shen Y., Strauss M. A., Richards G. T., Lunnan R., 2010, ApJ, 723, 1119
Lintott C. et al., 2011, MNRAS, 410, 166
Lu Y., Wang T., Zhou H., Wu J., 2007, AJ, 133, 1615
Maccacaro T., Gioia I. M., Wolter A., Zamorani G., Stocke J. T., 1988, ApJ, 326, 680
Mahabal A., Kembhavi A., McCarthy P. J., 1999, ApJ, 516, L61 (MKM99)
Masci F. J., Cutri R. M., Francis P. J., Nelson B. O., Huchra J. P., Heath Jones D., Colless M., Saunders W., 2010, Publ. Astron. Soc. Australia, 27, 302
Mauch T., Sadler E. M., 2007, MNRAS, 375, 931
Morić I., Smolčić V., Kimball A., Riechers D. A., Ivezić Ž, Scoville N., 2010, ApJ, 724, 779 (M10)
Nesvadba N. P. H., Lehnert M. D., De Breuck C., Gilbert A. M., van Breugel W., 2008, A&A, 491, 407
Oke J. B., Gunn J. E., 1983, ApJ, 266, 713
Osterbrock D. E., 1989, Astrophysics of Gaseous Nebulae and Active Galactic Nuclei. University Science Books, Mill Valley
Sadler E. M. et al., 2002, VizieR Online Data Catalog, 732, 90227
Schawinski K., Thomas D., Sarzi M., Maraston C., Kaviraj S., Joo S.-J., Yi S. K., Silk J., 2007, MNRAS, 382, 1415
Schawinski K. et al., 2009, ApJ, 690, 1672
Schlegel D. J., Finkbeiner D. P., Davis M., 1998, ApJ, 500, 525
Shabala S. S., Ash S., Alexander P., Riley J. M., 2008, MNRAS, 388, 625
Shin M., Strauss M. A., Tojeiro R., 2011, MNRAS, 410, 1583
Stoughton C., Lupton R. H. e. A., 2002, AJ, 123, 485
Strateva I., Ivezić Ž., Knapp G. e. A., 2001, AJ, 122, 1861
Strauss M. A. et al., 2002, ApJ, 124, 1810
Tadhunter C., Robinson T. G., González Delgado R. M., Wills K., Morganti R., 2005, MNRAS, 356, 480

Taylor M. B., 2005, in Shopbell P. L., Britton M. C., Ebert R., eds, ASP Conf. Ser. Vol. 347, Astronomical Data Analysis Software and Systems XIV. Astron. Soc. Pac., San Francisco, p. 29
van Breugel W., Fragile C., Croft S., de Vries W., Anninos P., Murray S., 2004, in Storchi-Bergmann T., Ho L. C., Schmitt H. R., eds, IAU Symp. 222, The Interplay Among Black Holes, Stars and ISM in Galactic Nuclei. Cambridge Univ. Press, Cambridge, p. 485
Vincent R. A., Ryden B. S., 2005, ApJ, 623, 137
Worrall D. M., 1989, in Hunt J., Battrick B., eds, ESA SP-296, The 23rd ESLAB Symp. on Two Topics in X-Ray Astronomy. Volume 1: X-Ray Binaries. Volume 2: AGN and the X-Ray Background. ESA Publications Division, Noordwijk, p. 719
Yan R., Newman J. A., Faber S. M., Konidaris N., Koo D., Davis M., 2006, ApJ, 648, 281
Yan R. et al., 2011, ApJ, 728, 38
York D. G. et al., 2000, AJ, 120, 1579
Yun M. S., Reddy N. A., Condon J. J., 2001, ApJ, 554, 803

This paper has been typeset from a TEX/LATEX file prepared by the author.